Chemical Science

ROYAL SOCIETY OF CHEMISTRY

EDGE ARTICLE

View Article Online
View Journal | View Issue

Cite this: *Chem. Sci.*, 2023, **14**, 6087

All publication charges for this article have been paid for by the Royal Society of Chemistry

Received 10th March 2023
Accepted 13th May 2023

DOI: 10.1039/d3sc01295f

rsc.li/chemical-science

From closed-shell edge-extended kekulenes to open-shell carbonylated cycloarene diradicaloid†

Dongdong Chang,‡ Jiangyu Zhu,‡ Yutao Sun, Kai Chi, Yanjun Qiao, Teng Wang, Yan Zhao, Yunqi Liu and Xuefeng Lu *

The precise synthesis of cycloarenes remains a challenging topic in both organic chemistry and materials science due to their unique fully fused macrocyclic π-conjugated structure. Herein, a series of alkoxyl- and aryl-cosubstituted cycloarenes (kekulene and edge-extended kekulene derivatives, **K1–K3**) were conveniently synthesized and an unexpected transformation of the anthryl-containing cycloarene **K3** into a carbonylated cycloarene derivative **K3-R** was disclosed by controlling the temperature and gas atmosphere of the $Bi(OTf)_3$-catalyzed cyclization reaction. All their molecular structures were confirmed by single-crystal X-ray analysis. The crystallographic data, NMR measurements, and theoretical calculations reveal their rigid quasi-planar skeletons, dominant local aromaticities, and decreasing intermolecular π–π stacking distance with extension of the two opposite edges. The much lower oxidation potential for **K3** by cyclic voltammetry explains its unique reactivity. Moreover, carbonylated cycloarene derivative **K3-R** shows a remarkable stability, large diradical character, a small singlet–triplet energy gap ($\Delta E_{S-T} = -1.81$ kcal mol^{-1}), and weak intramolecular spin–spin coupling. Most importantly, it represents the first example of carbonylated cycloarene diradicaloids as well as the first example of radical-acceptor cycloarenes and will shed some light on synthesis of extended kekulenes and conjugated macrocyclic diradicaloids and polyradicaloids.

Introduction

Cycloarenes are fully fused macrocycles with an enclosed cavity, by the combination of annellations of benzene units.[1] In the beginning, many theoretical studies focused on the question of their electron structure: whether π-electrons in cycloarenes are localized on sextets or delocalized throughout the whole conjugated skeleton,[2] until the first cycloarene kekulene, a regular hexagonal macrocycle consisting of 12 benzene rings, was successfully synthesized by Staab and Diederich in 1978.[3] The deshielded inner protons by ^{1}H NMR measurement suggest that π-electrons are localized on individual benzenoid rings, which supports the hypothesis proposed by McWheeny[2b] and the model described by Clar.[2c] In the following three decades, the single synthesis strategy and the poor solubility of products limited the development of cycloarenes,[4] and only a contracted kekulene cyclo[*d*,*e*,*d*,*e*,*e*,*d*,*e*,*d*,*e*,*e*]decakisbenzene was reported.[5] Recently, kekulene's seven-sided cousin septulene synthesized by ring-closing metathesis of olefins[6] and the alkoxy substituted octagonal cousin octulene prepared by the fold-in method were reported in 2012 and 2016, respectively.[7] Subsequently we and Wu's group developed an efficient synthetic strategy for aryl-substituted cycloarenes and alkoxy substituted hetero-cycloarenes through $Bi(OTf)_3$-catalyzed cyclization from a macrocyclic methoxyethenylated precursor.[8] In 2021, based on this strategy, Wu's group reported a series of core-expanded kekulenes, more than two edges of which are expanded.[9] Moreover, there are some peripherally fused kekulene analogues obtained by on-surface synthesis[10] or Diels–Alder cycloaddition in solution.[11] Although some effective synthetic strategies have been explored over the years, only a few cycloarenes were reported,[12] and the poor molecular diversity severely limited their further development.

Herein, according to the extension of phenyl building blocks from benzene to anthracene, we have successfully designed and synthesized an alkoxyl- and aryl-cosubstituted kekulene (**K1**) and its edge-extended homologues (**K2** and **K3**) by the Suzuki coupling reaction followed by $Bi(OTf)_3$-catalyzed cyclization of vinyl ethers at room temperature. Interestingly, a carbonylated cycloarene derivative **K3-R** with two anthroxyl radicals was obtained when we raised the temperature of the cyclization reaction to 80 °C under an air atmosphere, which displays open-shell singlet ground diradical character with a small singlet–triplet energy gap ($\Delta E_{S-T} = -1.81$ kcal mol^{-1}) verified by X-ray

Department of Materials Science, State Key Laboratory of Molecular Engineering of Polymers, Fudan University, Shanghai 200433, China. E-mail: luxf@fudan.edu.cn

† Electronic supplementary information (ESI) available: Synthetic procedures and characterization data of all physical characterization studies and theoretical calculations and additional spectroscopic data. CCDC 2223047–2223050. For ESI and crystallographic data in CIF or other electronic format see DOI: https://doi.org/10.1039/d3sc01295f

‡ D. C. and J. Z. contributed equally to this work.

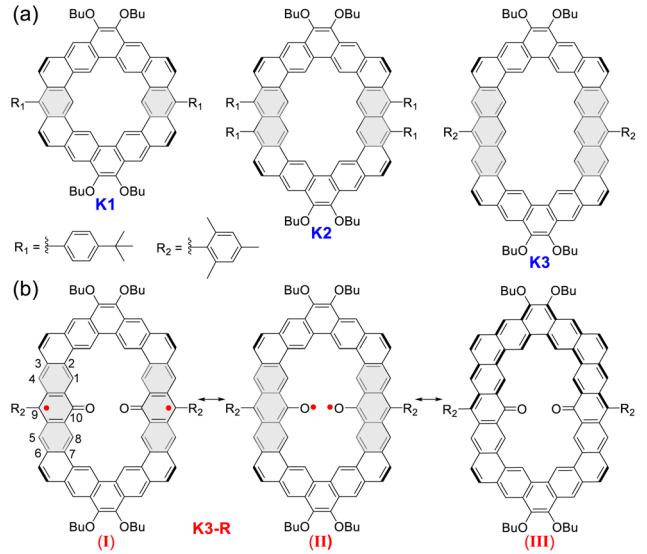

Fig. 1 (a) Structures of alkoxyl- and aryl-cosubstituted kekulene **K1** and its edge-extended homologues **K2** and **K3**. (b) The representative resonance forms of carbonylated cycloarene diradical **K3-R**.

crystallography and variable-temperature electron spin resonance (VT ESR) measurements. According to X-ray single crystal analysis, optical spectroscopy and theoretical calculations, we have systematically investigated the size-dependent molecular overlap model, electronic structure and aromaticity of these three closed-shell cycloarenes and the open-shell carbonylated cycloarene diradicaloid. The low oxidation potential for **K3** measured by cyclic voltammetry (CV) supports reasonable unique reactivity of anthryl-based cycloarene and facilitates the formation of diradical product **K3-R**. Meanwhile, **K3-R** can be drawn in at least three different resonance forms (Fig. 1):[13] an open-shell diradical form with the unpaired electron localized at the 9-position (I); an open-shell diradical form with the unpaired electron localized at oxygen atoms (II); and a closed-shell form containing a quinoidal and an aromatic dibenzo [*a*,*o*]pentaphene (III). Thus, the electronic structure, aromaticity, and radical character of open-shell anthroxyl-based macrocycle diradical **K3-R** are of great interest due to the contributions of multiple resonance forms. The crystallographic data reveals the dominant contribution of resonance structure I, and the theoretical calculations show its large radical character and weak intramolecular spin–spin coupling between the two neighboring spins.

Results and discussion

Synthesis

The synthesis of alkoxyl- and aryl-cosubstituted kekulene **K1** and its edge-extended homologues **K2** and **K3** was carried out as shown in Scheme 1. **K1** can be regarded as an aryl- and alkoxy-cosubstituted kekulene, and its tetramethoxyethenylated macrocyclic precursor **5** was synthesized by the Suzuki coupling reaction using XPhos Pd G2 as a catalyst[14] in 14.7% isolated yield, with benzene and phenanthrene units as building blocks.

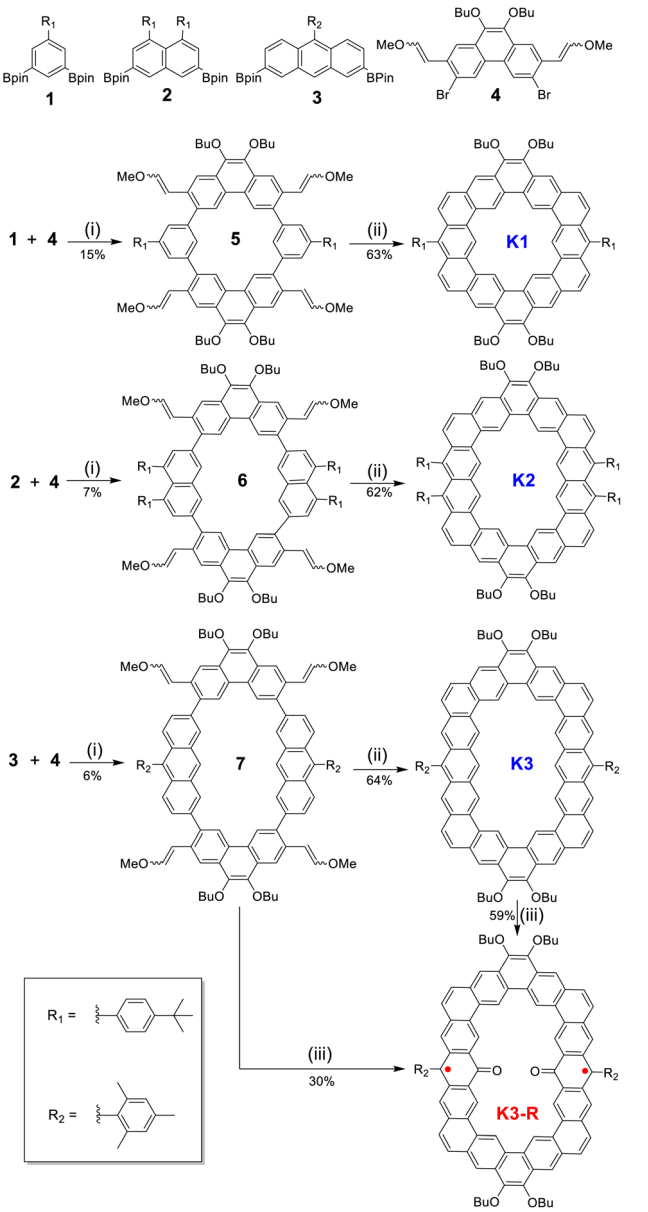

Scheme 1 Synthetic route of alkoxyl- and aryl-cosubstituted cycloarenes **K1**–**K3** and carbonylated cycloarene diradical **K3-R**: (i) XPhos Pd G2, K_3PO_4, THF/H_2O, 50 °C; (ii) $Bi(OTf)_3$, CH_2ClCH_2Cl, rt; (iii) $Bi(OTf)_3$, air (O_2), CH_2ClCH_2Cl, 80 °C.

Then, treatment of **5** with $Bi(OTf)_3$ catalyzed cyclization in 1,2-dichloroethane (DCE) at room temperature gave the fully fused product **K1** in 63% yield.[8,14,15] By the replacement of benzene units with naphthalene and anthracene units, the higher homologues **K2** and **K3** were synthesized as yellow and orange solids, respectively. All new products were characterized by NMR spectroscopy and high-resolution mass spectroscopy.

Interestingly, when heating a mixture of anthryl-based tetramethoxyethenylated macrocyclic precursor 7 and $Bi(OTf)_3$ in DCE at 80 °C under an air atmosphere, we obtain an anthroxyl-based diradical product **K3-R** as a black solid, which can be regarded as a carbonylated cycloarene derivative. It is stable enough to be purified over conventional flash silica gel column

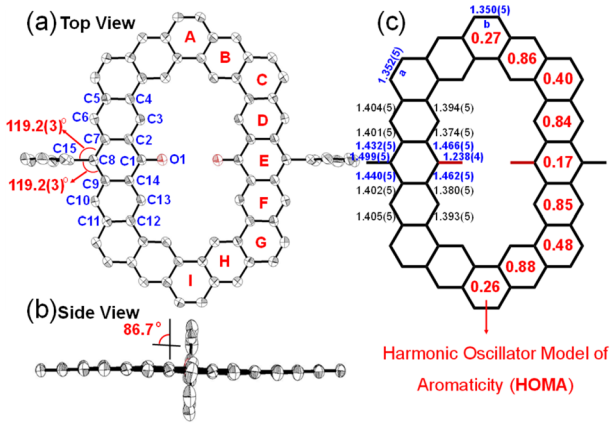

Fig. 2 X-ray crystallographic structure of **K3-R**: (a) top view with labels; (b) side view; (c) selected bond lengths (in Å) of the backbone. The numbers in parentheses are the estimated standard deviations (esds). The red numbers in rings A–I are the calculated HOMA values. Hydrogen atoms, alkyl, and alkoxy substituents are omitted for clarity.

chromatography (dichloromethane as an eluent). In the NMR spectrum, although sharp signals corresponding to the methyl protons and some CH_2 protons of the butoxyl group were observed, a broad resonance signal was observed in the aromatic region at room temperature, which suggests the paramagnetic character of **K3-R**. Even at −90 °C, the ^{1}H NMR signal of **K3-R** was still broad (Fig. S5†) indicating appreciable triplet character.[16] This product was identified by high-resolution mass spectrum measurement (Fig. S37†), single crystal X-ray diffraction analysis (Fig. 2) and ESR spectroscopy (Fig. S6† and 6a). It is worth noting that the diradical product **K3-R** can also be obtained directly by treating cycloarene **K3** under the same heating conditions, indicating that the transformation from **7** to **K3-R** involves both cyclization and oxidation. Generally, the oxidation of anthracene to an anthroxyl radical requires high reaction temperature (200–300 °C).[17] Meanwhile, in the absence of bismuth triflate, the oxidation of **7** or **K3** to diradical **K3-R** did not proceed, even under an air (O_2) atmosphere, which indicates that $Bi(OTf)_3$ may significantly reduce the activation energy of oxidation and the oxidation is the result of the combination of the bismuth(III) catalyst and O_2 as the oxidant.[18] Additionally, this oxidation was not observed in the benzene- or naphthalene-based macrocyclic system, indicating that this is the intrinsic nature of anthryl-based cycloarene.

X-ray crystallographic structure and aromaticity

The single crystals of three alkoxyl- and aryl-cosubstituted cycloarenes **K1**–**K3** were grown by slow diffusion of *n*-hexane into the carbon disulfide solution under ambient conditions. All three crystals are aligned in triclinic unit cells with the space group $P\bar{1}$. Their crystallographic structures are shown in Fig. 3, which clearly reveal slightly distorted coplanar π-conjugated skeletons. The hexagonal skeleton is stretched with the extension of the building block from benzene to anthracene, and the side length of zigzag edges connected to aryl-substituted groups is calculated to be 7.36 Å for **K1**, 9.84 Å for **K2** and 12.25 Å for **K3**

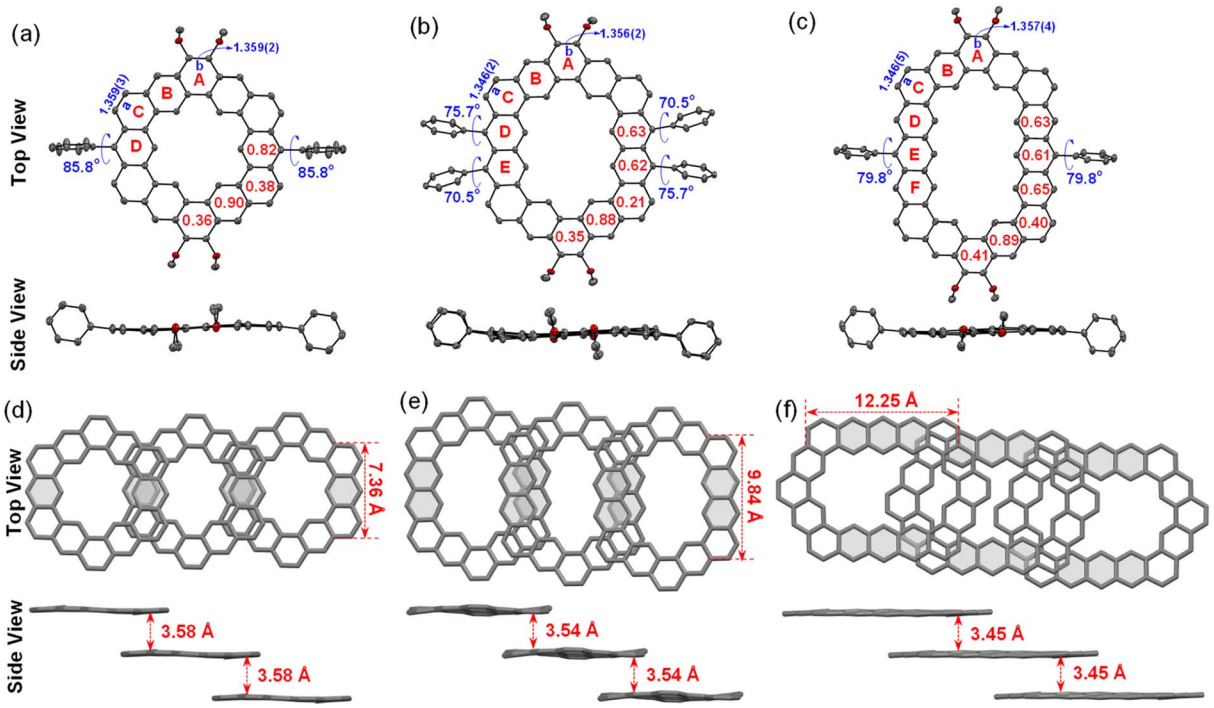

Fig. 3 Single-crystal X-ray diffraction structures (hydrogen atoms and alkyl substituents are omitted and the long alkoxy substituents are shortened to methoxy substituents for clarity), selected bond lengths (Å), calculated HOMA values, and crystal framework packing structures of (a and d) **K1**, (b and e) **K2**, and (c and f) **K3**.

(Fig. 3). Different from the herringbone pattern of kekulene with no substituent group,[19] alkoxyl- and aryl-cosubstituted **K1–K3** adopt a one-dimensional (1D) slipped stacking, and the interplanar distance decreases with extension of the two opposite edges. By creating planes based on all of the C atoms in skeletons, the interplanar distance was measured to be 3.58 Å for **K1**, 3.54 Å for **K2** and 3.45 Å for **K3** (Fig. 3). Meanwhile, with the replacement of the *t*-butylphenyl group with a larger steric hindrance mesityl group, the overlap of adjacent molecules concentrates from the aryl-substituted sides for **K1**/**K2** to the alkoxy-substituted sides for **K3**, which may facilitate tighter packing.

The single crystal of carbonylated cycloarene derivative **K3-R** was grown by slow diffusion of methanol into a $CHCl_3$ solution at room temperature and is shown in Fig. 2. The crystal of **K3-R** is aligned in a triclinic unit cell and there are two molecules of **K3-R** in each asymmetric unit, which is similar to its closed-shell precursor **K3**. The molecular backbone is rigid and slightly distorted and the molecular packing exhibits 1D parallel stacking with an intermolecular distance of 3.48 Å, which is a little wider than that of **K3**. The bond length of CO bonds at the 10-position of anthracene units of **K3-R** is 1.238(4) Å, which is almost as short as the ketone C=O bond length in benzophenone (1.23 Å),[20] and indicates their doubled bond characters. The C7–C8 (1.432(5) Å) and C8–C9 (1.440(5) Å) are longer than the C(sp^2)–C(sp^2) bond (1.39 Å) in benzene, and close to the typical C(sp^2)–C(sp^2) single-bond (1.46 Å),[20] which suggests its single-bond character. Moreover, the bond angles of ∠C15–C8–C7 (119.2(3)°) and ∠C15–C8–C9 (119.2(3)°) are near the sp^2 hybridization bond angle (120°), which verifies that the atom C8 is an sp^2 hybrid. The above crystallographic analysis suggests its carbonylated cycloarene structure containing two anthroxyl radicals. In addition, the lack of both significant bond length alternation and NMR signal at room temperature implies that the major resonance contribution of open-shell **K3-R** is form I as shown in Fig. 1.

To further understand the aromaticity of three closed-shell alkoxyl- and aryl-cosubstituted cycloarenes **K1–K3** and the open-shell carbonylated cycloarene derivative **K3-R**, the bond length analysis (Fig. 2, 3 and S1†), harmonic oscillator model of aromaticity (HOMA) calculations (Fig. 2 and 3),[21] nucleus independent chemical shift (NICS) (Fig. S1†),[22] anisotropy of the induced current density (ACID) (Fig. 4a–d),[23] and 2D isochemical shielding surface (ICSS) (Fig. 4e–h) calculations[24] were carried out. For the three closed-shell cycloarenes **K1–K3**, bond length analysis shows that the bond lengths of bonds *a* from vinyl ethers and the bonds *b* in phenanthrene units (1.346(2)–1.359(3) Å) are obviously shorter than that of the typical C(sp^2)–C(sp^2) bond (1.39 Å) in benzene[20] but close to that of typical olefins (1.34 Å),[25] indicating their double bond character. The small HOMA values (the numbers in red color) for individual rings also imply the weak aromaticity in the corresponding rings C and A (Fig. 3). The NICS(0) values (Fig. S1†) and ACID plots (Fig. 4a–c) display local aromatic character. The calculated 2D ICSS maps of **K1–K3** (Fig. 4e–g) indicate that the building blocks benzene/naphthalene/anthracene units exhibit strong magnetic shielding. All these analysis results suggest local aromatic character of the three closed-shell cycloarenes **K1–K3**, like the other cycloarenes,[12] and their π-electrons are mainly delocalized at the individual benzene/naphthalene/anthracene ring and the two periphery hexatomic rings of the phenanthrene unit. For the open-shell carbonylated cycloarene derivative **K3-R**, the bonds a and b show the same double bone character as that of its closed-shell parent **K3** (Fig. 2). The NICS(0) value of the center of the macrocycle is nearly zero (−0.88 ppm) exhibiting local aromatic character. Different from

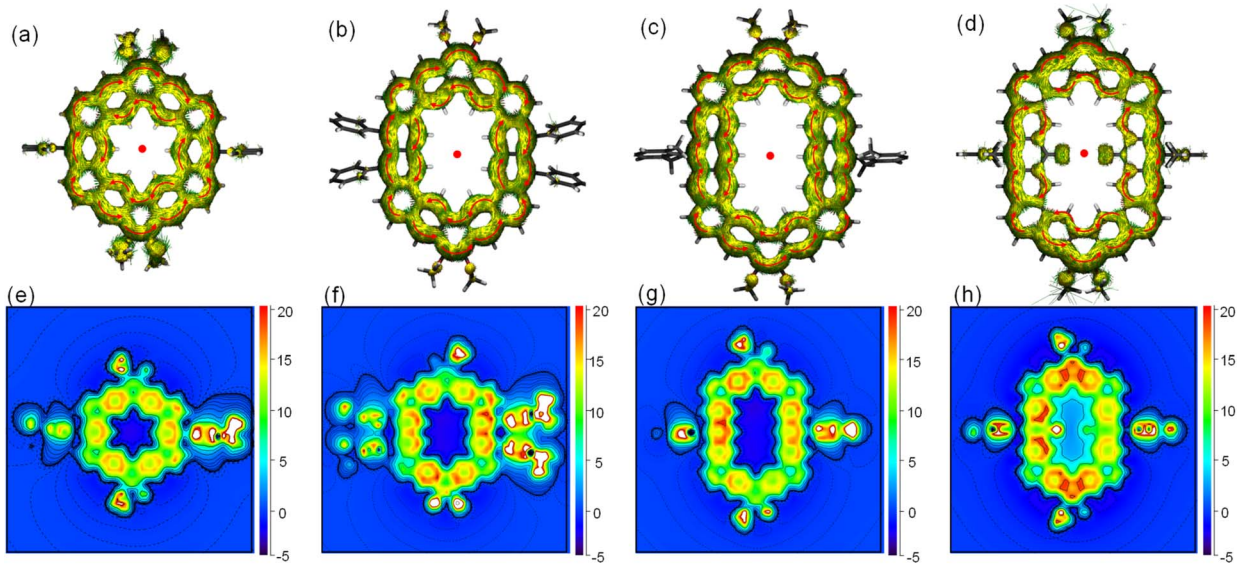

Fig. 4 Calculated ACID plots (contribution from π-electrons only) of (a) **K1**, (b) **K2**, (c) **K3**, and (d) **K3-R**. The magnetic field is perpendicular to the *XY* plane and points out through the paper. The red arrows indicate the clockwise (diamagnetic) current flow. Calculated 2D $ICSS_{zz}$ maps for (e) **K1**, (f) **K2**, (g) **K3**, and (h) **K3-R**.

the continuous ring currents over the anthracene units for **K3**, there is almost no ring current on the atom C1, indicating that the ring currents are mainly distributed in the outer rings of the anthroxyl structure, which is consistent with the 2D ICSS map (Fig. 4h). Meanwhile, compared with the three rings of the anthracene unit in **K3** with almost equal HOMA values (0.61–0.65), the HOMA value of the centered ring *E* (0.17) of the anthroxyl structure in **K3-R** is obviously smaller than that of the lateral rings D/F (0.84–0.85) (Fig. 2), which can be attributed to the relatively long bond lengths of C7–C8 and C8–C9 due to the conjugation with the carbonyl groups. Overall, the above calculations about aromaticity verify again that form I is the dominant resonance structure of open-shell carbonylated cycloarene derivative **K3-R**.

Optical and electrochemical properties

The UV-vis absorption spectra (Fig. 5a and b) and fluorescence emission spectra (Fig. S3†) of three closed-shell kekulene homologues **K1–K3** were measured in chloroform as shown in Fig. 5a. With the major absorption at 330 nm and several shoulder peaks at 352 nm and 397 nm, the band structure of aryl- and alkoxy-cosubstituted kekulene **K1** is similar to that of aryl-substituted kekulene[9] and alkoxy-substituted kekulene.[7] The absorption maxima (λ_{max}) of **K2** and **K3** bathochromic shift to 360 nm and 382 nm, respectively, compared with that of **K1** (λ_{max} = 330 nm), which can be explained using the extended π-conjugation system. The absorption bands at 400–500 nm for **K2** and 460–610 nm for **K3** resemble the characteristics of the tetracene[26] and pentacene moiety,[27] respectively, which can be assigned a combination of HOMO → LUMO electronic transitions according to the time-dependent (TD) DFT calculations (see the ESI†). The optical energy gap (E_g^{opt}) of **K1–K3** was estimated to be 3.01 eV, 2.50 eV and 2.25 eV, respectively, from the UV-vis absorption edge (Fig. 5a). Moreover, the red-shift from the expanded conjugation was also observed in the fluorescence spectra (Fig. S3†). The absolute fluorescence quantum yields of **K1–K3** in chloroform solution were measured to be 7.3%, 13.8% and 31.7%, respectively, by using the integrating sphere technique. The absorption spectrum of carbonylated cycloarene derivative **K3-R** shows a weak long wavelength absorption band with λ_{max} = 625 nm along with a shoulder at 750 nm extending up to 850 nm, which is a typical character observed in many compounds with unpaired electrons.[28] According to TD DFT, the NIR absorption can originate from HOMO-5 → LUMO and HOMO → LUMO+3 (Fig. S14 and Table S4†). The optical energy gap of **K3-R** was estimated to be 1.51 eV at the onset absorption wavelength. The stability of **K3-R** in $CHCl_3$ at room temperature under ambient air and light conditions was also monitored by UV-vis measurements (Fig. S8†). The absorption intensity at 506 nm decreased by only 34% in about 97 days, indicating that **K3-R** is significantly more stable than other reported cycloarene-based radicals.[29] Meanwhile, the superior stability of **K3-R** supports that the attachment of electron-acceptor groups is an efficient approach toward stable open-shell cycloarene diradicaloids and polyradicaloids. Moreover, there is no fluorescence detected for the solid or the solution of the carbonylated cycloarene derivative **K3-R**.

Cyclic voltammetry (CV) and differential pulse voltammetry (DPV) measurements of **K1–K3** and **K3-R** were performed in dry DCM by using 0.1 M tetra-*n*-butylammonium hexfluorophosphate as the supporting electrolyte (Fig. 5 and S4†). Similar to other cycloarenes, **K1** and **K2** are difficult to oxidize because of their high first oxidation potential.[9] However, a low oxidation potential with a half-wave $E_{1/2}^{ox}$ of 0.29 V (*vs.* Fc^+/Fc) of anthryl-based cycloarene **K3** was observed, which can explain its unique reactivity.[30] DFT calculations were performed using Gaussian 09 at the B3LYP/6-31G(d,p) level to investigate the electronic properties of **K1–K3** by using simplified model molecules.[31] As shown in Fig. S10,† the frontier molecular orbitals of **K1–K3** were delocalized over the whole aromatic backbone, but the larger electron cloud density at five fused benzenoid rings was observed in **K3**, which was consistent with the observed pentacene-like band structure in the absorption spectrum. The electrochemical properties of carbonylated cycloarene derivative **K3-R** were investigated by the same method with the above closed-shell molecules, and two reversible oxidation waves with $E_{1/2}^{ox}$ = 0.01 and 0.19 V and one reduction wave with $E_{1/2}^{red}$ = −0.97 V (*vs.* Fc^+/Fc) were observed. The HOMO/LUMO energy levels of **K3-R** were determined to be −4.72/−3.93 eV from the onset of the first oxidation/reduction potential, and the electrochemical energy gap (E_g^{EC}) was estimated to be 0.79 eV.

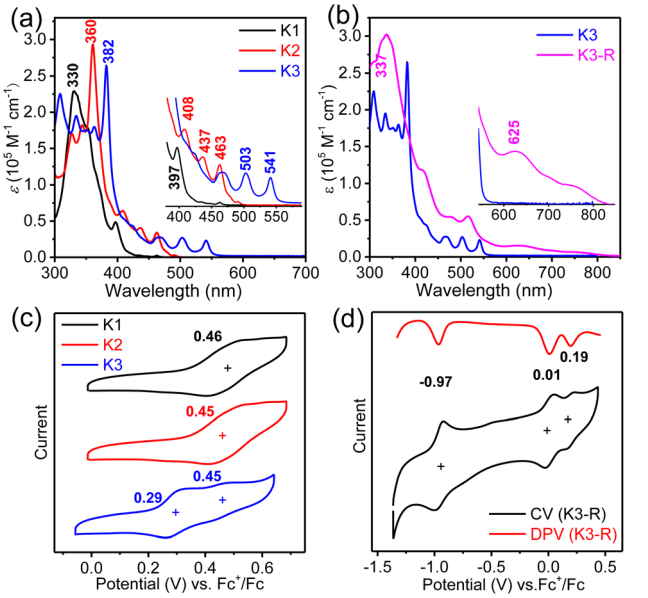

Fig. 5 UV-vis absorption spectra of (a) **K1–K3** and (b) **K3-R** in chloroform solutions; insets show the magnified onset absorption bands. Cyclic voltammograms of (c) **K1–K3** and (d) **K3-R** in chloroform solutions.

Magnetic properties and radical character

The magnetic properties of **K3-R** were further investigated by variable-temperature (VT) ESR measurements in a solid (Fig. 6a). The signal intensity decreased as the temperature

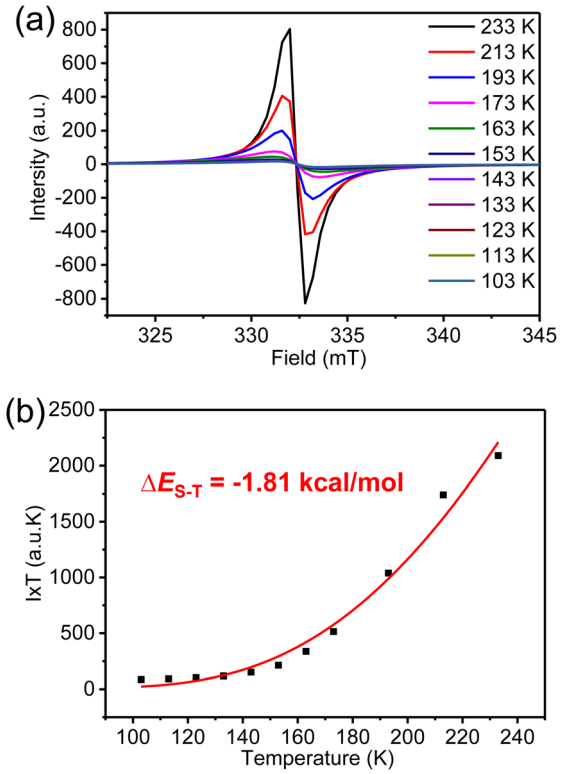

Fig. 6 (a) VT ESR spectra and (b) fitted $I \times T$–T curves by using the Bleaney–Bowers equation of carbonylated cycloarene diradical **K3-R** in a solid.

was lowered, indicating the open-shell singlet diradical character of **K3-R**. By fitting the data using the Bleaney–Bowers equation (Fig. 6b),[32] the singlet–triplet energy gap (ΔE_{S-T}) was calculated to be −1.81 kcal mol^{-1}. However, the broad resonance signals in ^{1}H NMR spectra of **K3-R** were observed at room temperature and even after cooling to 183 K (Fig. S5†). Indeed, the diradical character (y_0)[33] of **K3-R** was calculated to be 92% at the UCAM-B3LYP/6-31G(d,p) level, which can indicate its strong radical character and explain the broad NMR signals even at low temperature. The diradical character and excitation energies of **K3-R** were calculated at the unrestricted B3LYP/6-31G(d,p) level. The excitation energy from the singlet ground state to the lowest triplet was estimated to be 0.32 kcal mol^{-1}. The natural orbital profiles and spin density distribution map of **K3-R** are shown in Fig. 8 and S15.† The unpaired electron density and spin density were mainly delocalized over anthroxyl units and thinly distributed in other areas of the macrocycle skeleton, suggesting the weak antiferromagnetic (AFM) coupling between the two spin centers. This weak intramolecular spin–spin coupling and the steric protection of the reactive carbon atom are effective in stabilizing anthroxyl type radicals.

Conclusions

In summary, an alkoxyl- and aryl-cosubstituted kekulene **K1** and its homologues **K2** and **K3** with extensions of the two opposite edges were designed and synthesized successfully. Then, an interesting transition from the closed-shell anthryl-based cycloarene **K3** to open-shell carbonylated cycloarene derivative **K3-R** was found *via* controlling the temperature and gas atmosphere of the Bi(OTf)$_3$-catalyzed system. The unique reactivity of anthryl-based cycloarene **K3** can be attributed to its low oxidation potential of 0.29 V (*vs.* Fc$^+$/Fc). All their molecular structures and quasi-planar skeleton geometry were confirmed by X-ray crystallographic analysis. Clear size-dependent physical properties and crystal packing modes can be observed for this unique closed-shell cycloarene system. Most importantly, carbonylated cycloarene derivative **K3-R** exhibits intramolecular AFM coupling, large diradical character, small singlet–triplet energy gap, and remarkable stability and represents the first example of carbonylated cycloarene diradicaloids. Our studies disclose the distinct reactivity of alkoxyl- and aryl-cosubstituted kekulene and its edge-extended homologues, further enriching our understanding of the electronic properties of cycloarenes, and shed some light on synthesis of extended kekulenes and conjugated radical-acceptor cycloarenes.

Data availability

The crystallographic data was provided in Cambridge Structural Database, and the other necessary data of this study have been provided in the ESI.†

Author contributions

X. L. supervised the project. X. L. and D. C. designed the experiments and performed all the synthetic experiments and characterization. X. L. and J. Z. analyzed the data, performed theoretical calculations and co-wrote the manuscript. Y. S., K. C., Y. Q., and T. W. assisted in the synthesis of compounds. Y. Z. Y. L. and X. L. discussed the results and commented on the manuscript.

Conflicts of interest

There are no conflicts to declare.

Acknowledgements

This work was financially supported by the National Natural Science Foundation of China (52073063, 51903052, and 61890940), the National Key R&D Program of China (2018YFA0703200), the Natural Science Foundation of Shanghai (22ZR1405800, and 23ZR1405100), and the Program for Professor of Special Appointment (Eastern Scholar) at the Shanghai Institutions of Higher Learning.

Notes and references

1 H. A. Staab, F. Diederich, C. Krieger and D. Schweitzer, *Chem. Ber.*, 1983, **116**, 3504–3512.

2 (*a*) L. Pauling, *J. Chem. Phys.*, 1936, **4**, 673–677; (*b*) R. McWeeny, *Proc. Phys. Soc. A*, 1951, **64**, 921–930; (*c*) E. Clar, *The Aromatic Sextet*, J. Wiley, New York, 1972.
3 F. Diederich and H. A. Staab, *Angew. Chem., Int. Ed. Engl.*, 1978, **17**, 372–374.
4 (*a*) E. F. Jenny and A. Melzer, *Angew. Chem., Int. Ed. Engl.*, 1965, **4**, 951–952; (*b*) R. Peter and W. Jenny, *Helv. Chim. Acta*, 1966, **49**, 2123–2135; (*c*) H. A. Staab, F. Diederich and V. Čaplar, *Liebigs Ann. Chem.*, 1983, **1983**, 2262–2273; (*d*) H. A. Staab and M. Sauer, *Liebigs Ann. Chem.*, 1984, **1984**, 742–760.
5 D. J. H. Funhoff and H. A. Staab, *Angew. Chem., Int. Ed. Engl.*, 1986, **25**, 742–744.
6 B. Kumar, R. L. Viboh, M. C. Bonifacio, W. B. Thompson, J. C. Buttrick, B. C. Westlake, M.-S. Kim, R. W. Zoellner, S. A. Varganov, P. Mörschel, J. Teteruk, M. U. Schmidt and B. T. King, *Angew. Chem., Int. Ed.*, 2012, **51**, 12795–12800.
7 M. A. Majewski, Y. Hong, T. Lis, J. Gregoliński, P. J. Chmielewski, J. Cybińska, D. Kim and M. Stępień, *Angew. Chem., Int. Ed.*, 2016, **55**, 14072–14076.
8 (*a*) W. Fan, Y. Han, S. Dong, G. Li, X. Lu and J. Wu, *CCS Chem.*, 2021, **3**, 1445–1452; (*b*) M. Murai, N. Hosokawa, D. Roy and K. Takai, *Org. Lett.*, 2014, **16**, 4134–4137; (*c*) L. Yang, N. Zhang, Y. Han, Y. Zou, Y. Qiao, D. Chang, Y. Zhao, X. Lu, J. Wu and Y. Liu, *Chem. Commun.*, 2020, **56**, 9990–9993.
9 W. Fan, Y. Han, X. Wang, X. Hou and J. Wu, *J. Am. Chem. Soc.*, 2021, **143**, 13908–13916.
10 M. Di Giovannantonio, X. Yao, K. Eimre, J. I. Urgel, P. Ruffieux, C. A. Pignedoli, K. Müllen, R. Fasel and A. Narita, *J. Am. Chem. Soc.*, 2020, **142**, 12046–12050.
11 U. Beser, M. Kastler, A. Maghsoumi, M. Wagner, C. Castiglioni, M. Tommasini, A. Narita, X. Feng and K. Müllen, *J. Am. Chem. Soc.*, 2016, **138**, 4322–4325.
12 J. C. Buttrick and B. T. King, *Chem. Soc. Rev.*, 2017, **46**, 7–20.
13 (*a*) T. Aotake, M. Suzuki, N. Aratani, J. Yuasa, D. Kuzuhara, H. Hayashi, H. Nakano, T. Kawai, J. Wu and H. Yamada, *Chem. Commun.*, 2015, **51**, 6734–6737; (*b*) Y. Hirao, A. Konishi and T. Kubo, *Org. Chem. Front.*, 2017, **4**, 828–833; (*c*) V. W. Manner, T. F. Markle, J. H. Freudenthal, J. P. Roth and J. M. Mayer, *Chem. Commun.*, 2008, 256–258; (*d*) Y. Hirao, T. Saito, H. Kurata and T. Kubo, *Angew. Chem., Int. Ed.*, 2015, **54**, 2402–2405; (*e*) F. Miao, Z. L. Lim, P. Hu, S. Dong, Q. Qi, X. Zhang and J. Wu, *Org. Biomol. Chem.*, 2017, **15**, 3188–3191.
14 (*a*) J. Zhu, W. Li, N. Zhang, D. An, Y. Zhao, X. Lu and Y. Liu, *Chem. Sci.*, 2022, **13**, 11174–11182; (*b*) N. Zhang, L. Yang, W. Li, J. Zhu, K. Chi, D. Chang, Y. Qiao, T. Wang, Y. Zhao, X. Lu and Y. Liu, *J. Am. Chem. Soc.*, 2022, **144**, 21521–21529.
15 (*a*) W. Fan, T. Matsuno, Y. Han, X. Wang, Q. Zhou, H. Isobe and J. Wu, *J. Am. Chem. Soc.*, 2021, **143**, 15924–15929; (*b*) N. Zhang, J. Zhu, D. An, R. Zhang, X. Lu and Y. Liu, *Org. Lett.*, 2022, **24**, 5439–5443.
16 (*a*) M. Abe, *Chem. Rev.*, 2013, **113**, 7011–7088; (*b*) A. Shimizu, R. Kishi, M. Nakano, D. Shiomi, K. Sato, T. Takui, I. Hisaki, M. Miyata and Y. Tobe, *Angew. Chem., Int. Ed.*, 2013, **52**, 6076–6079; (*c*) Z. Zeng, X. Shi, C. Chi, J. T. López Navarrete, J. Casado and J. Wu, *Chem. Soc. Rev.*, 2015, **44**, 6578–6596; (*d*) W. Zeng, H. Phan, T. S. Herng, T. Y. Gopalakrishna, N. Aratani, Z. Zeng, H. Yamada, J. Ding and J. Wu, *Chem*, 2017, **2**, 81–92; (*e*) A. Konishi, Y. Hirao, K. Matsumoto, H. Kurata, R. Kishi, Y. Shigeta, M. Nakano, K. Tokunage, K. Kamada and T. Kubo, *J. Am. Chem. Soc.*, 2013, **135**, 1430–1437; (*f*) H. Hayashi, J. E. Barker, A. Cárdenas Valdivia, R. Kishi, S. N. MacMillan, C. J. Gómez-García, H. Miyauchi, Y. Nakamura, M. Nakano, S. Kato, M. M. Haley and J. Casado, *J. Am. Chem. Soc.*, 2020, **142**, 20444; (*g*) A. Shimizu, T. Kubo, M. Uruichi, K. Yakushi, M. Nakano, D. Shiomi, K. Sato, T. Takui, Y. Hirao, K. Matsumoto, H. Kurata, Y. Morita and K. Nakasuji, *J. Am. Chem. Soc.*, 2010, **132**, 14421; (*h*) J. J. Dressler and M. M. Haley, *J. Phys. Org. Chem.*, 2020, **33**, e4114.
17 I. C. Lewis and L. S. Singer, *J. Phys. Chem.*, 1981, **85**, 354–360.
18 (*a*) S. Antoniotti and E. Duñach, *Eur. J. Org. Chem.*, 2004, **2004**, 3459–3464; (*b*) T. Zevaco, E. Duñach and M. Postel, *Tetrahedron Lett.*, 1993, **34**, 2601–2604; (*c*) K. Kallal, C. Coin, E. Dunach and M. Postel, *New J. Chem.*, 1997, **21**, 495–502.
19 C. Krieger, F. Diederich, D. Schweitzer and H. A. Staab, *Angew. Chem., Int. Ed. Engl.*, 1979, **18**, 699–701.
20 E. Fleischer, N. Sung and S. Hawkinson, *J. Phys. Chem.*, 1968, **72**, 4311–4312.
21 (*a*) J. Kruszewski and T. M. Krygowski, *Tetrahedron Lett.*, 1972, **13**, 3839–3842; (*b*) T. M. Krygowski, *J. Chem. Inf. Comput. Sci.*, 1993, **33**, 70–78.
22 Z. Chen, C. S. Wannere, C. Corminboeuf, R. Puchta and P. R. Schleyer, *Chem. Rev.*, 2005, **105**, 3842–3888.
23 (*a*) D. Geuenich, K. Hess, F. Köhler and R. Herges, *Chem. Rev.*, 2005, **105**, 3758–3772; (*b*) T. Luo, Y. Wang, J. Hao, P. Chen, Y. Hu, B. Chen, J. Zhang, K. Yang and Z. Zeng, *Angew. Chem., Int. Ed.*, 2023, **62**, e202214653.
24 (*a*) S. Klod and E. Kleinpeter, *J. Chem. Soc., Perkin Trans. 2*, 2001, 1893–1898; (*b*) T. Lu and F. Chen, *J. Comput. Chem.*, 2012, **33**, 580–592.
25 R. Glaser, L. Dendi, N. Knitts and C. Barnes, *Cryst. Growth Des.*, 2003, **3**, 291–300.
26 S. A. Odom, S. R. Parkin and J. E. Anthony, *Org. Lett.*, 2003, **5**, 4245–4248.
27 (*a*) Y. Kawanaka, A. Shimizu, T. Shinada, R. Tanaka and Y. Teki, *Angew. Chem., Int. Ed.*, 2013, **52**, 6643–6647; (*b*) A. Maliakal, K. Raghavachari, H. Katz, E. Chandross and T. Siegrist, *Chem. Mater.*, 2004, **16**, 4980–4986; (*c*) I. Kaur, W. Jia, R. P. Kopreski, S. Selvarasah, M. R. Dokmeci, C. Pramanik, N. E. McGruer and G. P. Miller, *J. Am. Chem. Soc.*, 2008, **130**, 16274–16286.
28 (*a*) X. Lu, S. Lee, J. O. Kim, T. Y. Gopalakrishna, H. Phan, T. S. Herng, Z. Lim, Z. Zeng, J. Ding, D. Kim and J. Wu, *J. Am. Chem. Soc.*, 2016, **138**, 13048–13058; (*b*) X. Lu, T. Y. Gopalakrishna, Y. Han, Y. Ni, Y. Zou and J. Wu, *J. Am. Chem. Soc.*, 2019, **141**, 5934–5941.
29 (*a*) X. Lu, D. An, Y. Han, Y. Zou, Y. Qiao, N. Zhang, D. Chang, J. Wu and Y. Liu, *Chem. Sci.*, 2021, **12**, 3952–3957; (*b*) S. Das, T. S. Herng, J. L. Zafra, P. M. Burrezo, M. Kitano, M. Ishida,

T. Y. Gopalakrishna, P. Hu, A. Osuka, J. Casado, J. Ding, D. Casanova and J. Wu, *J. Am. Chem. Soc.*, 2016, **138**, 7782–7790; (*c*) X. Lu, T. Y. Gopalakrishna, H. Phan, T. S. Herng, Q. Jiang, C. Liu, G. Li, J. Ding and J. Wu, *Angew. Chem., Int. Ed.*, 2018, **57**, 13052–13056; (*d*) H. Gregolińska, M. Majewski, P. J. Chmielewski, J. Gregoliński, A. Chien, J. Zhou, Y.-L. Wu, Y. J. Bae, M. R. Wasielewski, P. M. Zimmerman and M. Stępień, *J. Am. Chem. Soc.*, 2018, **140**, 14474–14480.

30 S. H. Jang, T. B. Tai, M. K. Kim, J. W. Han, Y. H. Kim, S. C. Shin, Y. J. Yoon, S. K. Kwon and S. G. Lee, *Bull. Korean Chem. Soc.*, 2009, **30**, 618–622.

31 M. J. Frisch, G. W. Trucks, H. B. Schlegel, G. E. Scuseria, M. A. Robb, J. R. Cheeseman, G. Scalmani, V. Barone, B. Mennucci, G. A. Petersson, H. Nakatsuji, M. Caricato, X. Li, H. P. Hratchian, A. F. Izmaylov, J. Bloino, G. Zheng, J. L. Sonnenberg, M. Hada, M. Ehara, K. Toyota, R. Fukuda, J. Hasegawa, M. Ishida, T. Nakajima, Y. Honda, O. Kitao, H. Nakai, T. Vreven, J. A. Montgomery Jr, J. E. Peralta, F. Ogliaro, M. Bearpark, J. J. Heyd, E. Brothers, K. N. Kudin, V. N. Staroverov, T. Keith, R. Kobayashi, J. Normand, K. Raghavachari, A. Rendell, J. C. Burant, S. S. Iyengar, J. Tomasi, M. Cossi, N. Rega, J. M. Millam, M. Klene, J. E. Knox, J. B. Cross, V. Bakken, C. Adamo, J. Jaramillo, R. Gomperts, R. E. Stratmann, O. Yazyev, A. J. Austin, R. Cammi, C. Pomelli, J. W. Ochterski, R. L. Martin, K. Morokuma, V. G. Zakrzewski, G. A. Voth, P. Salvador, J. J. Dannenberg, S. Dapprich, A. D. Daniels, O. Farkas, J. B. Foresman, J. V. Ortiz, J. Cioslowski and D. J. Fox, *Gaussian 09 Rev. C.01*, Gaussian, Inc., Wallingford, CT, 2010.

32 (*a*) B. Bleaney and K. D. Bowers, *Proc. R. Soc. London, Ser. A*, 1952, **214**, 451–465; (*b*) B. Li, C. Yang, X. Wang, G. Li, W. Peng, W. Peng, H. Xiao, S. Luo, S. Xie, J. Wu and Z. Zeng, *Angew. Chem., Int. Ed.*, 2021, **60**, 19790; (*c*) Y. Wang, Y. Huang, T. Huang, J. Zhang, T. Luo, Y. Ni, B. Li, S. Xie and Z. Zeng, *Angew. Chem., Int. Ed.*, 2022, **61**, e202200855.

33 T. Minami and M. Nakano, *J. Phys. Chem. Lett.*, 2012, **3**, 145–150.